International Journal of Trend in Scientific Research and Development (IJTSRD)
Volume 5 Issue 3, March-April 2021 Available Online: www.ijtsrd.com e-ISSN: 2456 – 6470

CFD Analysis on Forced Convection Heat Transfer of KNO_3–Ca $(NO_3)_2$ + TiO_2 Molten Salt Nanofluid in Circular Tube

Prof. Om Prakash[1], Sourav Raj[2]

[1]Assistant Professor, [2]Research Scholar,
[1,2]Corporate Institute of Science and Technology, RGPV Bhopal, Madhya Pradesh, India

ABSTRACT

Nanotechnology has been a global movement in recent decades. The possibility of manipulating atomic and molecular materials has resulted in previously unimaginable properties and characteristics. The molten salt nanofluid created by integrating nanoparticles into molten salt has a much higher specific heat capacity and thermal conductivity than the base molten salt, resulting in a higher heat storage density and lower heat storage cost than the base molten salt. Since the discovery of molten salt nanofluid's excellent thermal properties, the heat transfer of molten salt nanofluid has piqued engineers' curiosity. In this analysis, the forced convection heat transfer of KNO_3–Ca $(NO3)_2$ + TiO2 molten salt nanofluid in circular tube was investigated using a 3-dimensional numerical (3-D) simulation. The simulation programme ANSYS 17.0 was used for study of the heat transfer physiognomies of a KNO_3–Ca $(NO3)_2$ + TiO2 molten salt nanofluid in circular tube. The effect of nanofluid were measured and observed to influence the heat transfer and flow of fluids in a heat exchanger. The following conclusions can be drawn based on the provided results: The KNO_3–Ca $(NO_3)_2$ + TiO_2 molten salt nanofluid performed slightly better in forced convection heat transfer than the KNO_3–Ca $(NO_3)_2$ + SiO_2 molten salt nanofluid under the same working conditions. KNO_3–Ca $(NO_3)_2$ + TiO_2 molten salt nanofluid had a 14.79 percent higher Nusselt number than KNO_3–Ca $(NO_3)_2$ + SiO_2 molten salt nanofluid.

KEYWORDS: *Nanofluids, Molten Salts, Reynold's number, Heat transfer, Nusselt Number, CFD*

How to cite this paper: Prof. Om Prakash | Sourav Raj "CFD Analysis on Forced Convection Heat Transfer of KNO3–Ca (NO3)2 + TiO2 Molten Salt Nanofluid in Circular Tube" Published in International Journal of Trend in Scientific Research and Development (ijtsrd), ISSN: 2456-6470, Volume-5 | Issue-3, April 2021, pp.450-460, URL: www.ijtsrd.com/papers/ijtsrd39853.pdf

IJTSRD39853

I. INTRODUCTION

Renewable energy sources such as wind, solar, geothermal, biomass, and waterpower are becoming increasingly relevant in our country's energy mix. The Department of Energy (DOE) aims to develop and rapidly commercialize clean energy technology. The Ministry is investing in renewable energy technologies that improve the economic and environmental performance by lowering carbon emissions and accelerating solar technology growth as a source of energy to the nation and to the planet. Solar energy is the most plentiful of the many renewable sources.

Due to the erratic nature of solar radiation, the most efficient use of this energy source necessitates the use of a Thermal Energy Storage (TES) system. The TES system acts as an energy reservoir, collecting and transferring thermal energy from the Heat Transfer Fluid (HTF) to storage media. There is a wide range of devices available to harness solar energy and use it for room and water heating, as well as power generation. The solar collector, the energy storage facility, and the steam generator used by the turbine-electric generator are the three main components of solar thermal energy utilization systems. Thermal energy is usually obtained using a parabolic trough, transported to thermal storage using a heat transfer fluid, and then transferred to a steam generator using storage media. The heat transfer fluid absorbs solar heat and acts as a storage medium in a direct device for active thermal energy storage.

Water is the most common heat transfer fluid for most industrial applications. The thermal energy is highly latent, the thermal conductivity is high, heat is highly specific and the viscosity is moderate. The main disadvantage of water as a heat transfer fluid is that it can be used for the small temperature ranges. The theoretical fluid range of water is between 0 and 100 °C but due to high vapor pressure near the boiling point; the practical temperature range for water used for heat transfer fluid is well under 100 °C.High pressure is also required if the temperature is higher than 100 °C and the associated pressure vessels and pipes are responsible for keeping the water in a fluid condition. As a heat transfer fluid or thermal energy medium, high temperature water (over 100 °C) for solar power plants is therefore unsuitable.

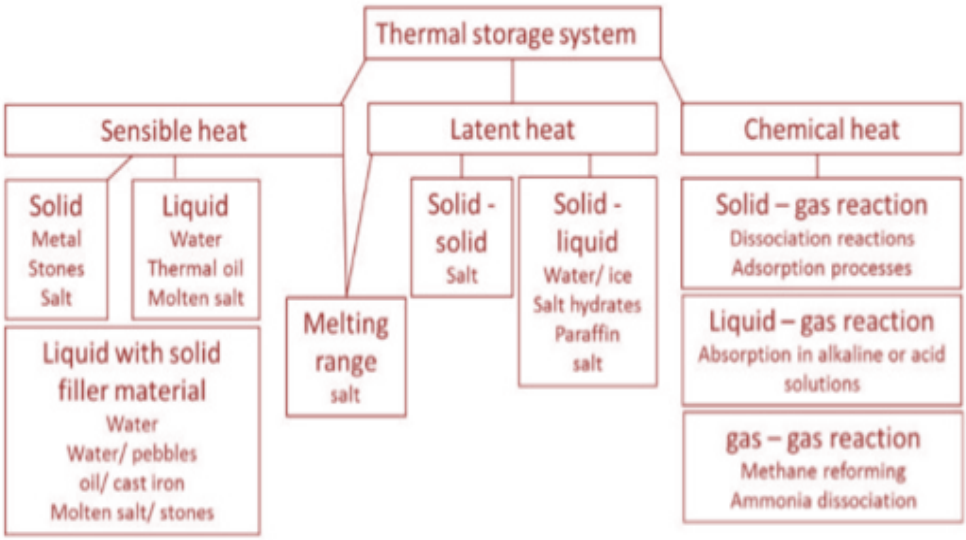

Figure 1 Methods for storing solar thermal energy

The use of thermal oils in the thermal storage media or heat transport fluid is possible up to 300°C in its liquid phase, but there are many intrinsic disadvantages, such as a low decomposition temperature, low density, flammability, high vapor pressure, a fuming ten dance and a poor chemical stability, which restrict their applications.

Molten salts are a very unique category with an enormous potential for storage and heat transmission media for solar energy applications, from the whole range of materials searched for different properties. For high temperatures from 250 °C to 1000 °C, molten salts were suggested as heat transfer fluids. Molten salts are a series of salts that remain liquid over a large range of temperatures. Other main LMP salts features include strong electrical and heat conductivity, high thermal and chemical stability, low viscosity and ecological performance. In the other hand, its low rate of heat transfer decreases its industrial efficiency. Improved thermo-physical properties (specific heat, c_p and thermal conductivity, k) are crucial to advancing the CSP systems of TES and current HTFs.

Recent studies have shown that molten salt Nano fluid formed by adding nanoparticles in molten salt may have a significantly greater basic thermal potential and thermal conductivity than its base molten salt. Research on molten salt Nano-fluid forced convection heat transfer is therefore insufficient.

II. LITERATURE REVIEW

Due to their stability at elevated temperatures, low vapor pressures, broad operating temperature ranges, minimal environmental footprint, ease of materials handling, low materials costs, and safety, research activities involving molten salts have gained popularity as working fluids for high temperature processing applications and thermal-fluidics applications over the last two decades. Solar power generation, advanced nuclear reactors, chemical refining, and energy storage are just some of the uses of molten salts as engineering fluids. Concentrating Solar Power (CSP) plants, in particular, are gaining prominence around the world.

Given the growing prevalence of molten salts in the contemporary research literature, the aim of this analysis is to elucidate the complexities of experimental heat transfer studies involving molten salts. The aim of this analysis is to objectively examine the observations in the literature and address their consequences. The aim of this analysis is to define potential research needs and directions based on discussions and consequences of previous literature findings. As a consequence, a list of recent developments concerning molten salt mixtures or eutectics (including a short overview of patterns in their thermo-physical properties) is presented.

Recent experimental findings involving forced convection heat transfer for molten salt eutectics are reviewed in this study with the aim of determining potential research directions and technological needs.

Bin et al. (2009) conducted turbulent convective heat transfer experiments using LiNO3 in a stainless steel concentric tube. Molten $LiNO_3$ flowing through the inner tube was cooled by flowing mineral oil through the annulus. The predictions from Dittus-Boelter and Colburn equation were higher than the experimental data, by as much as 25% and 18%, respectively [1].

Yang et al. (2010) investigated the heat transfer enhancement accruing from using a spiral tube instead of a smooth tube for receiver tubes in a Concentrated Solar Power (CSP) plant receiver. A ternary nitrate eutectic of KNO_3–$NaNO_2$–$NaNO_3$ (Hitec salt at 53:7:40 by mass fraction) was the working fluid. The authors also used a heated 316L Stainless Steel spiral tube as the test section. The experimental results indicate that the heat transfer performance can be enhanced by as much as 3 times in a spiral tube, in comparison to that of a smooth tube, for Reynolds number ranging from 15,000 to 55,000 [2].

Lu et al. (2013) performed a series of forced convective heat transfer experiments to investigate the efficacy of both spirally grooved and transversely grooved tubes compared to that of smooth tubes. The working fluid was Hitec salt. The test section was fabricated using stainless steel tubes. In general, both transverse and spiral grooves enhanced heat transfer by as much as ~1.4 times and ~1.5 times, respectively (compared to that of smooth tubes) for Reynolds number ranging from 5000 to 15000 [3].

Chen et al. (2016) investigated the heat transfer performance of Hitec salt in a salt-to-oil concentric tube heat exchanger with hot salt flowing through the inner tube being cooled by oil flowing in the outer tube. The Reynolds number on the molten salt side ranged from 10,000 to 50,000 and the Prandtl number ranged from 11 to 27. The experimental results indicate the measured heat transfer coefficient on the molten salt side were within ± 7% of the values predicted by the Gnielinski correlation and within ± 8% from the values predicted by the Sider-Tate correlation in fully turbulent regime [4].

Du et al. (2017) investigated the heat transfer performance of Hitec salt in transitional flow regime in a shell and tube heat exchanger with segmented baffles. The molten salt was pumped through the shell side and around the tube bundles with cooling oil flowing through the tubes. The measured heat transfer coefficient on the molten salt side agreed with traditional Kern correlation with a maximum deviation of 7.1% [5].

Hu et al. (2017) investigated the natural convection heat transfer of eutectic binary nitrate salt-based Al_2O_3 molten salt nanofluids in solar power systems. The result shows that the nanofluids with a 1.0% mass concentration of Al_2O_3 nanoparticles exhibit the best heat transfer performance [6].

Qian et al. (2017) studied the heat transfer performance of Hitec salt in a gas cooled shell and tube heat exchanger (finned tubes) with salt flowing internally through the tubes. The tests ranged from laminar flow to transition flow regimes (Reynolds number ranged from 987 to 12,000) and Prandtl number ranged from 9.8 to 18.9. The experimental data for Nusselt number was found to be within ± 15% of the predicted values [7].

To enhance the heat transfer performance, **Chen et al. (2018)** modified the experimental apparatus of (Chen et al., 2016) by replacing the inner tube with a transversely grooved tube. The hot salt flowing through the transversely grooved inner tube was cooled by oil flowing through the outer tube. The Reynolds number on the salt side ranged from 300 to 60,000 and Prandtl number ranged from 11 to 27. The authors reported 60% enhancement in the values of the heat transfer for the grooved tubes compared to that of the smooth tubes. However, measurements were not performed for determining the level of increase in pumping power due to the introduction of the grooves [8].

He et al. (2019) performed experiments to investigate the heat transfer performance of Hitec salt in a shell-and-tube heat exchanger without baffles. These experiments were performed by varying the inlet temperatures and flow velocities. The molten salt was pumped in the shell (i.e., external to the tube bundle) with effective Reynolds number ranging from 400 to 2300. Preheated water was pumped through the seven tubes. The measured values of Nusselt number on the molten salt side ranged from 20 to 100 based on the hydraulic diameter of the flow channel (which is computed based on the area of cross-section and the wetted perimeter).The experimental heat transfer coefficient on the molten salt side was found to be 3–5 times of the values predicted from the Sider-Tate correlation. The heat transfer enhancement was attributed to the thin developing boundary layer due to the tube bundle structure in the shell side [9].

Hu Chen et al. (2020) the forced convection heat transfer experiments were carried out in a circular tube of a previously reported promising molten salt nanofluid composed of KNO_3–Ca $(NO3)_2$ + 1 wt% of 20 nm SiO_2 nanoparticles (K-C-S_{nm}). Results showed that compared with its base pure molten salt, the K-C-S_{nm} molten salt nanofluid exhibited substantially better forced convection heat transfer performance under the same working condition. The Nusselt number and the convective heat transfer coefficient of K-C-S_{nm} molten salt nanofluid were 16.3% and 39.9% higher than its base pure molten salt, respectively [10].

Although the aforementioned researchers have researched different aspects of molten salts, there has been no study on forced convection heat transfer of molten salt nanofluid. However, such research is needed for the successful application of molten salt nanofluid in industrial practice. The forced convection heat transfer of molten salt nanofluid was numerically explored in this work.

III. GEOMETRY SETUP AND MODELLING

In this analysis, the forced convection heat transfer of KNO_3–Ca $(NO3)_2$ + TiO2 molten salt nanofluid in circular tube was investigated using a 3-dimensional numerical (3-D) simulation. The simulation programme ANSYS 17.0 was used for study of the heat transfer physiognomies of a KNO_3–Ca $(NO3)_2$ + TiO2 molten salt nanofluid in circular tube.

The geometry for performing simulation analysis is taken from **Hu Chen et al. (2020)**, a research scholar. Fig. 5.1 presents the schematic of the experimental system; a molten salt nanofluid circulation loop and a heat conduction oil circulation loop make up the majority of the system. The heat is transferred from molten salt nanofluid to heat conduction oil through a circular tube style heat exchanger in this experimental method.The design of the heat exchanger is shown in Fig. 5.2. The length of the heat exchanger tube L is 100 cm. The outer diameter $d_o$and inner diameter $d_i$of the heat exchange tube are 3.4 cm and 2 cm, respectively. The inner cross sectional area of the heat exchanger tube A_i is 3 cm^2, and the outer cross sectional area of the heat exchanger tube A_o is 9 cm^2. Molten salt is drained from a high-temperature tank, flows through a heat exchanger, and then flows back to the tank after going through a flow meter in the molten salt distribution loop. The oil is pumped from a constant temperature oil tank, passes through the heat exchanger, and then flows back into the oil tank after going through a radiator and a flow meter in the heat conduction oil-circulating loop.

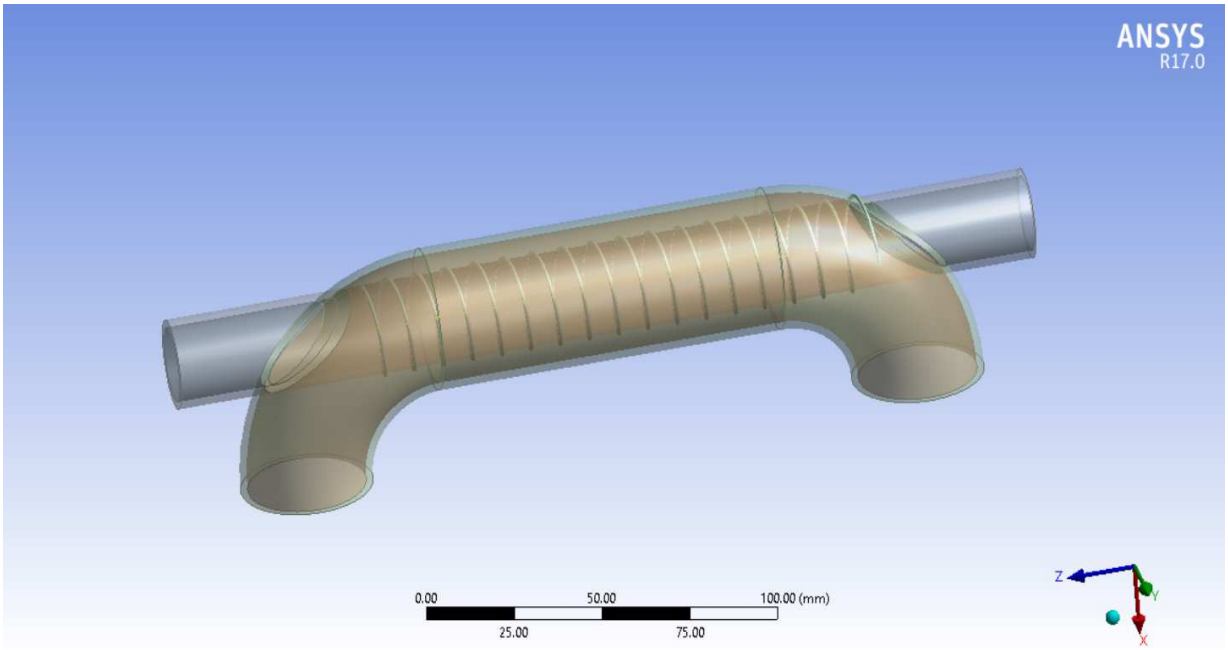

Figure 2 Computational model of heat exchanger

A three-dimensional discretized model was built in the pre-processor phase of ANSYS FLUENT R 17.0. Although the grid types are related to simulation results, the structure as a whole is, by necessity, discrete in the final volume; the programme ANSYS produces a coarse mesh. Mesh comprises unit-size mixed cells (ICEM Tetrahedral cells) with triangular frontier faces. In this analysis, a mesh metric is used with a medium fluid curvature.

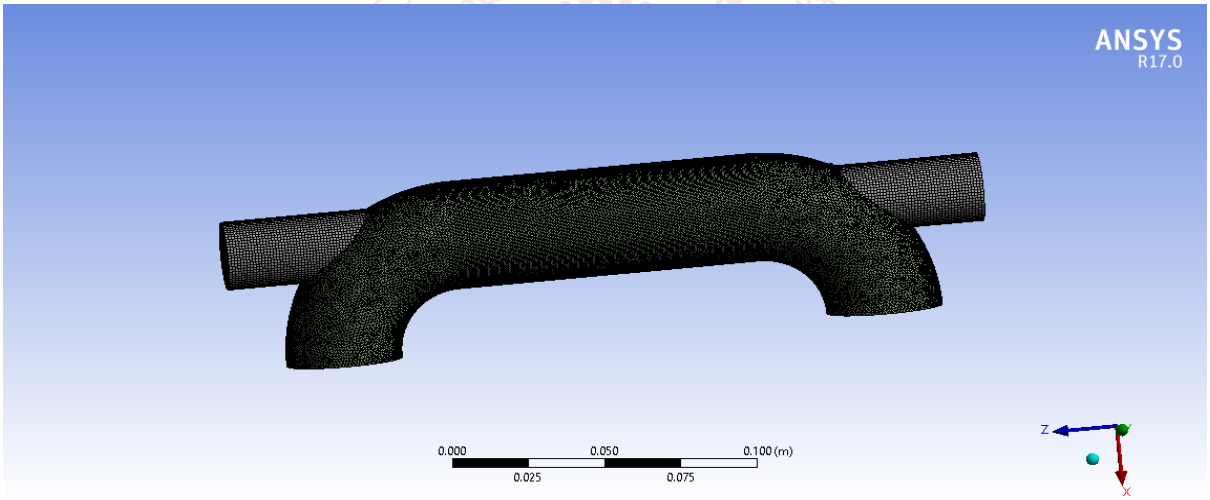

Figure 3 Meshing of heat exchanger

Table 1 Meshing detail of model

S. No.	Parameters	
1	Curvature	On
2	Smooth	Medium
3	Number of nodes	468775
4	Number of elements	1538922
5	Mesh metric	None
6	Meshing type	Tetrahedral

The Fluent 17.0 was used to calculate computationally. In research, the approach used to differentiate the governing equations was a finite element. For this convective term, the researchers used a simpler algorithm, and for connecting calculations of the pressure and velocity the second order upwind method was implemented.

A standard k-epsilon equation was used with flow and energy equations to solve turbulence.

Which implies the following hypotheses:

1. There is negligence of thermal radiation and normal convection;
2. The average of fluid and solid properties is calculated
3. Flow is incompressible;
4. Heat transfer steady state;
5. Transitional fluid flow and turbulent regimes, and
6. The fluid is distributed uniformly between the channels and the inlet channels have a uniform velocity profile.

The numerical simulation was with a 3-Dimensional steady state turbulent flow system. In order to solve the problem, governing equations for the flow and conjugate transfer of heat were customized according to the conditions of the simulation setup. The governing equations for mass, momentum, energy, turbulent kinetic energy and turbulent energy dissipation are expressed as follow,

Mass:

$$\frac{\partial(\rho u_i)}{\partial x_i} = 0$$

Momentum:

$$\frac{\partial(\rho u_i u_k)}{\partial x_i} = \frac{\partial\left(\mu \frac{\partial u_k}{\partial x_i}\right)}{\partial x_i} - \frac{\partial p}{\partial x_k}$$

Energy Equation:

$$\frac{\partial(\rho u_i t)}{\partial x_i} = \frac{\partial\left(\frac{K}{C_p}\frac{\partial t}{\partial x_i}\right)}{\partial x_i}$$

Table 2 Thermodynamic Properties of Binary Salt and Nano-particles

Input Parameters	Symbols	Units	Binary Salt	SiO_2	TiO_2
Specific heat capacity	c_p	J/kg-K	1.497	680	686.2
Density	ρ	(kg/m^3)	1.835	2220	4250
Thermal conductivity	k	W/m-K	0.55	1.3	8.593

Here the effective properties of the SiO_2/Molten Salt and TiO_2/Molten Salt nanofluid are defined as follows:

Pak and cho [11], **Patel** [12] and **Ebrahmnia- Bajestan** [29] suggested the below equations for determining density, thermal conductivity, specific heat and viscosity of nanofluids.

$$\rho_{nf} = \emptyset_p \rho_p + (1 - \emptyset_p)\rho_{bf}$$

$$(\rho C_p)_{nf} = (1 - \emptyset_p)(\rho C_p)_{bf} + \emptyset_p (\rho C_p)_p$$

$$K_{nf} = K_{bf}\left\{\frac{K_p + 2K_{bf} - 2\emptyset_p(K_{bf} - K_p)}{K_p + 2K_{bf} + \emptyset_p(K_{bf} - K_p)}\right\}$$

$$\mu_{nf} = \frac{\mu_{bf}}{(1 - \emptyset)^{2.5}}$$

Table 3 Thermodynamic Properties of KNO_3–$Ca(NO_3)_2$ + 1 wt% of 20 nm SiO_2 and KNO_3–$Ca(NO_3)_2$ + 1 wt % of 20 nm TiO_2 nanoparticles

Input Parameters	Symbols	Units	KNO3–Ca(NO3)2 + 1 wt % of 20 nm SiO2	KNO3–Ca(NO3)2 + 1 wt % of 20 nm TiO2
Specific heat capacity	c_p	J/kg-K	628.694	658.1323
Density	ρ	(kg/m^3)	24.016	44.31665
Thermal conductivity	k	W/m-K	0.555	0.5638

The discrete flow domain has been defined under sufficient limits. Inlets were allocated the mass flow rate requirements, while pressure outlet limits were allocated for outlets. The surfaces of the heat exchanger is regarded as normal wall limits. The interior walls were fitted with couplings of thermal walls.

Table 4 Details of boundary conditions

Detail	Value
Molten salt nanofluid flow rate	At different Reynold's no. 15000, 25000, and 35000
Heat conduction oil flow rate	0.465 kg/s
Molten salt nanofluid inlet temperature	300 °C
Heat conduction oil inlet temperature	125 °C
Outer surfaces	Heat flux=0

IV. RESULTS AND DISCUSSIONS

This section is aimed at evaluating the heat exchanger thermal performance using nanofluids. The variations in the Heat transfer rate and Thermal conductance are measured at different Reynold's number in order to research the performance of the heat exchanger using nanofluids subject to flow.

4.1. Data reduction equations

The values of Nusselt number, and Heat transfer coefficient calculated from the CFD modeling On the basis of temperature of hot and cold fluid obtained were compared with the values obtained from the analysis performed by **Hu Chen et al. (2020)**.

The data reduction of the measured results is summarized in the following procedures:

The Reynolds number is given by,

$$Re = \frac{\rho V D}{\mu}$$

The mass flow rate is calculate on the basis of below formula,

$$\dot{m} = \rho A V$$

Where, ρ is the density of fluid, A is the cross sectional area of the pipe and V is the velocity of fluid.

Therefore, for fluid flows in a concentric tube heat exchanger, the heat transfer rate of the hot fluid in the outer tube can be expressed as:

$$q_h = \dot{m}_h c_{ph}(T_{hi} - T_{ho})$$

Where $\dot{m}_h$ is the mass flow rate of hot fluid, c_{ph} is the specific heat of hot fluid, T_{hi} and T_{ho} are the inlet and outlet temperatures of hot fluid, respectively.

While, the heat transfer rate of the cold fluid in the inner tube can be expressed as:

$$q_c = \dot{m}_c c_{pc}(T_{co} - T_{ci})$$

Average heat transfer rate is given by:

$$Q_{avg} = \frac{q_h + q_c}{2} = UA\theta_m$$

Where, $\theta_m = \frac{\theta_1 - \theta_2}{2}$

θ_m is the logarithmic mean temperature difference.

U is the overall heat transfer coefficient.

Calculation of Nusselt Number,

$$Nu = \frac{\frac{f}{2}(Re - 1000)Pr}{1 + 12.7\left(\frac{f}{2}\right)^{0.5}\left(Pr^{\frac{2}{3}} - 1\right)}$$

Where, $f = [1.58\, ln(Re) - 3.82]^{-2}$

$$Pr = \frac{\mu c_p}{K}$$

$f \rightarrow friction\ factor$

$Nu \rightarrow Nusselt\ number$

$Pr \rightarrow Prandtl\ number$

4.2. Validation of numerical computations

To validate the accuracy of developed numerical approach, comparison was made with the work reported in **Hu Chen et al. (2020)**. The heat exchanger geometry that used for validation of numerical computations was considered as same as the geometry shown in Fig.3.

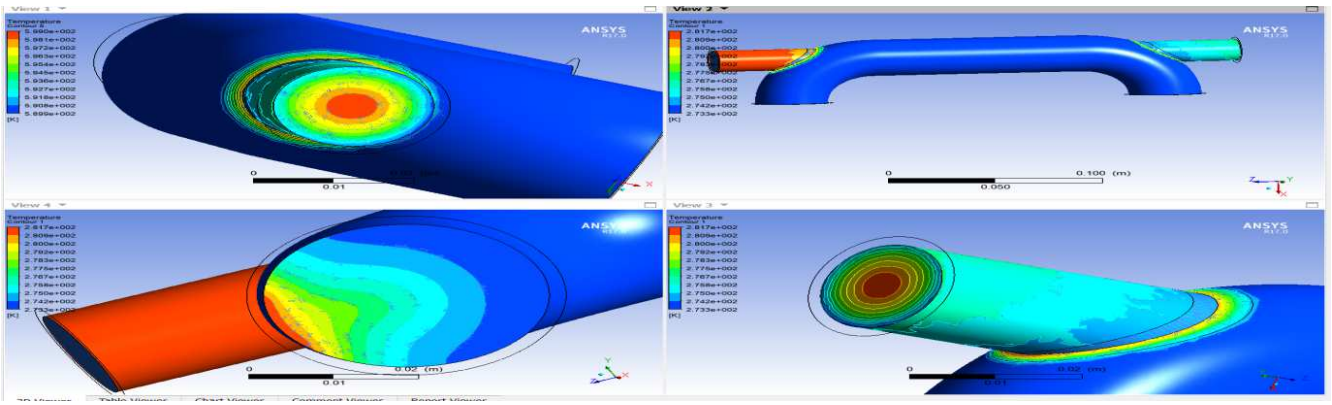

Figure 4 Temperature contour at Re = 15000 for heat exchanger using KNO_3–Ca $(NO3)_2$ + SiO2 molten salt nanofluid in a circular tube

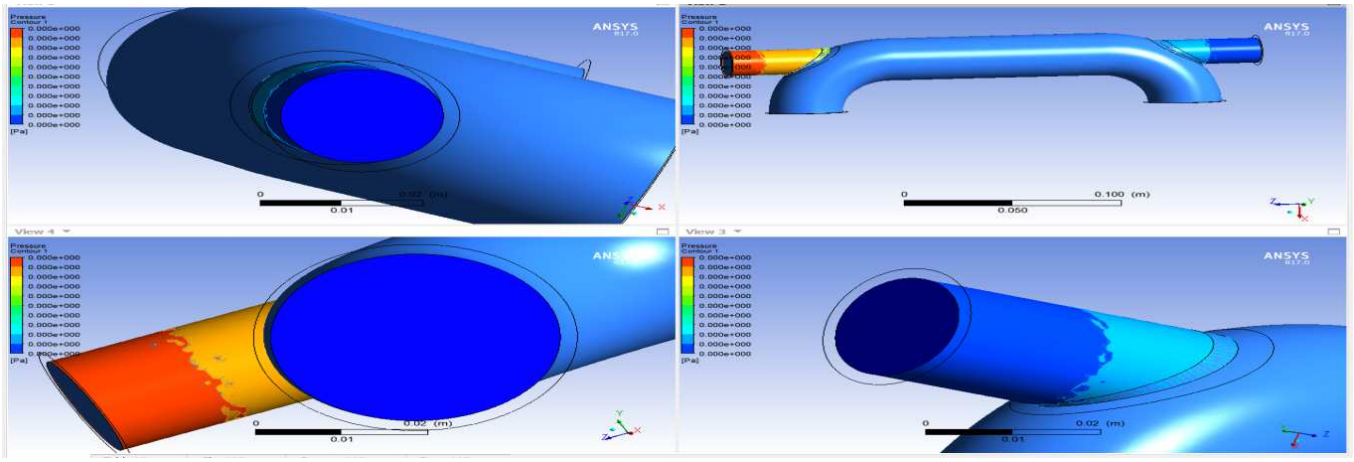

Figure 5 Pressure contour at Re = 15000 for heat exchanger using KNO_3–Ca $(NO3)_2$ + SiO2 molten salt nanofluid in a circular tube.

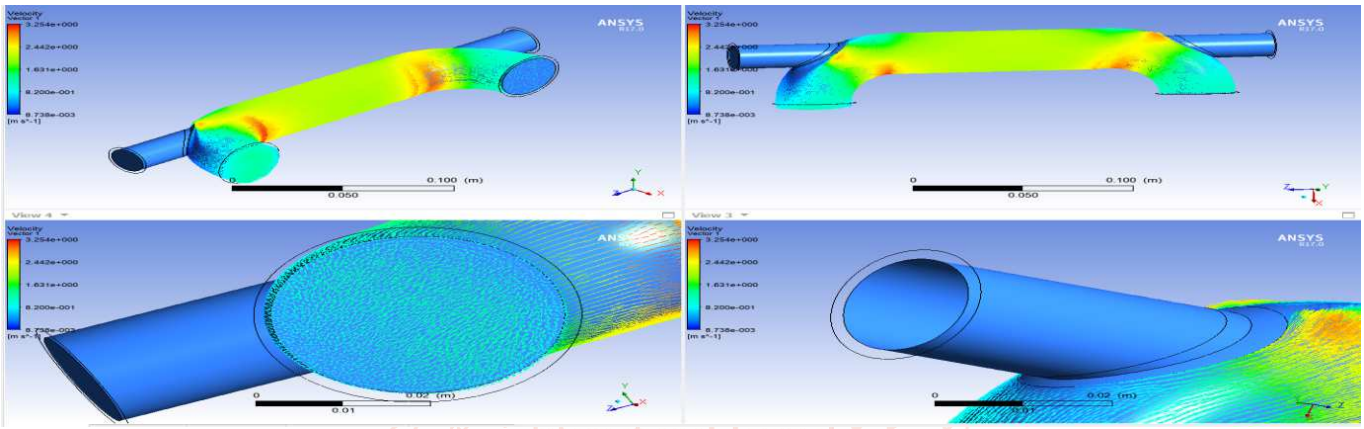

Figure 6 Velocity contour at Re = 15000 for heat exchanger using KNO_3–Ca $(NO3)_2$ + SiO2 molten salt nanofluid in a circular tube

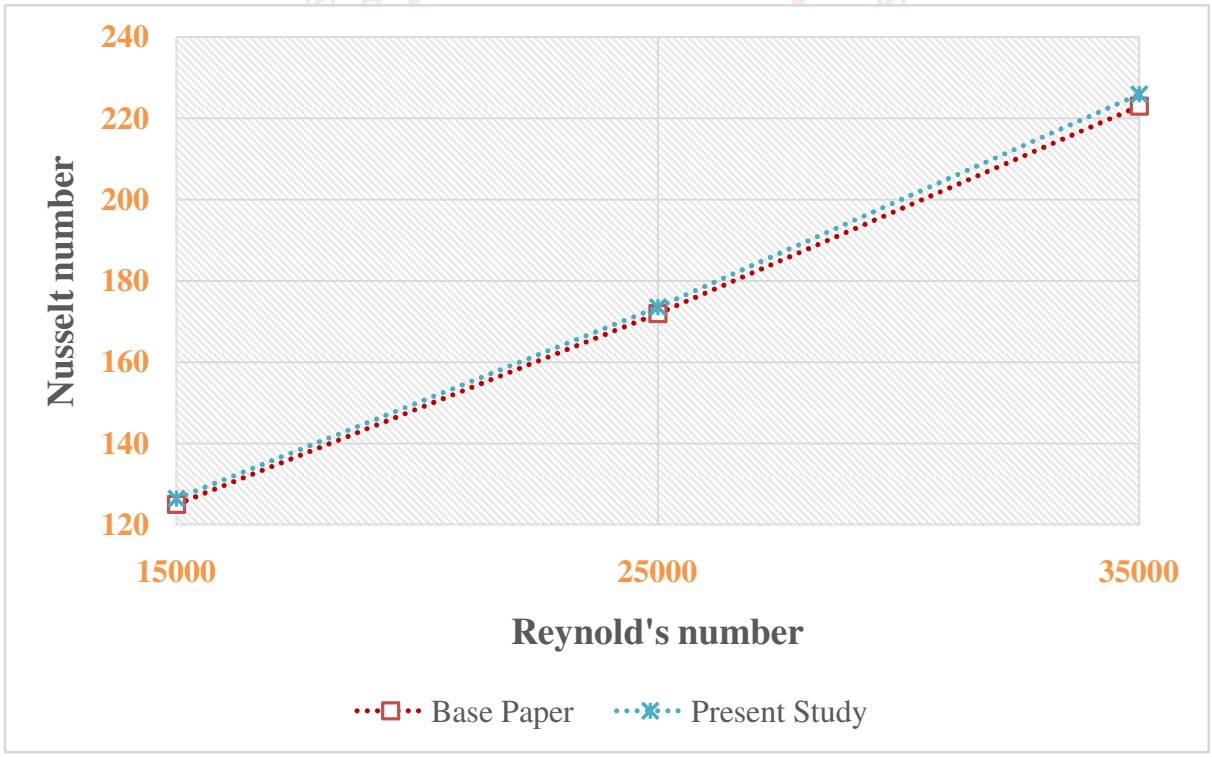

Figure 7 Values of Nusselt number calculated from the CFD modeling compared with the values obtained from the analysis performed by Hu Chen et al. (2020) for heat exchanger

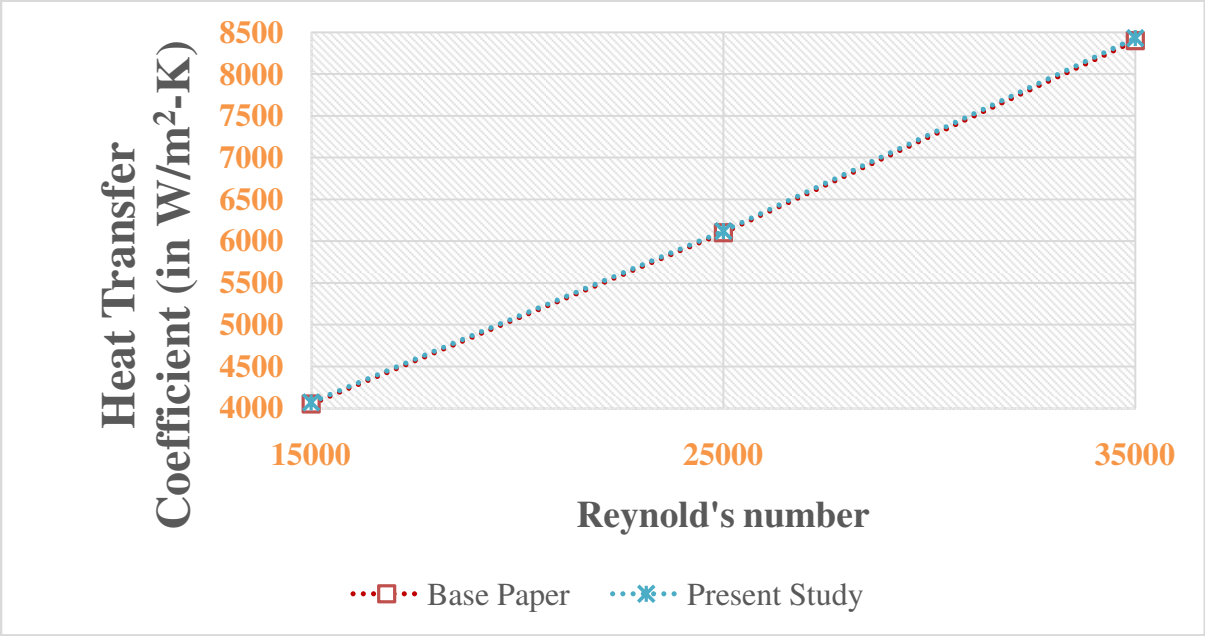

Figure 8 Values of Heat transfer coefficient calculated from the CFD modeling compared with the values obtained from the analysis performed by Hu Chen et al. (2020) for heat exchanger

From the above graph, it is found that the value of Nu number and heat transfer coefficient calculated from numerical analysis is closer to value of Nu number and heat transfer coefficient obtained from the base paper, which means that numerical model of heat exchanger using nanofluid, is correct. There is much lesser difference between experimental and numerical values.

4.3. Effect of suspension of TiO2 Nano-particles in the molten salt

From the numerical results and experimental data, it is seen that variation tendencies in the values of Nusselt number and heat transfer coefficient are qualitatively consistent. Therefore, to analyzing the effect of suspension of TiO_2Nano-particles in the molten salt to enhance thermal augmentation, we take volume concentration of 1 %. The boundary conditions were same as considered during the analysis of heat exchanger. The thermal properties of Nano fluids is mention in chapter 5, for calculating the effect of different Nano particles on Nusselt number, and heat transfer coefficient.

- **For Re = 15000**

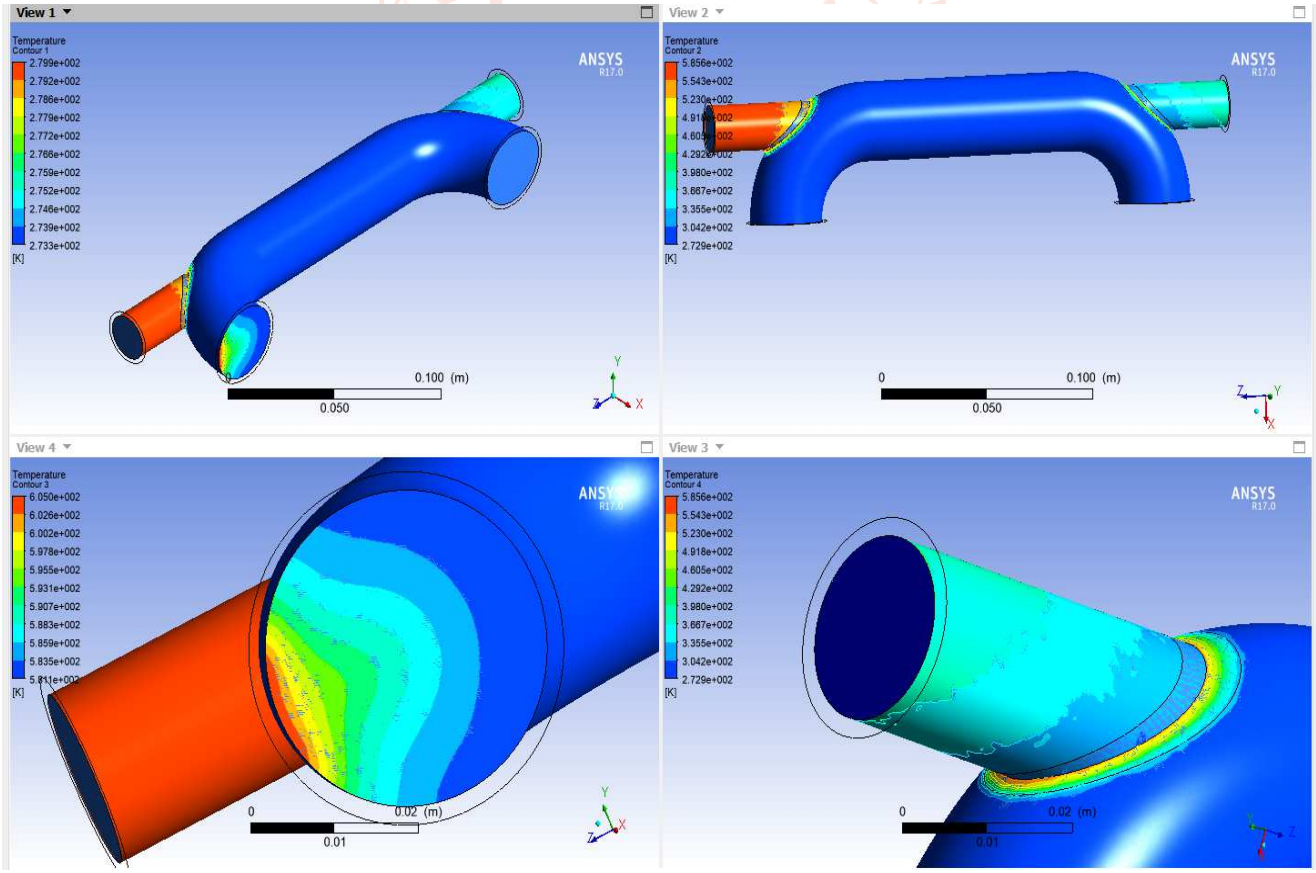

Figure 9 Temperature contour at Re = 15000 for heat exchanger using KNO_3–Ca $(NO3)_2$ + TiO2 molten salt nanofluid in a circular tube.

- **For Re = 25000**

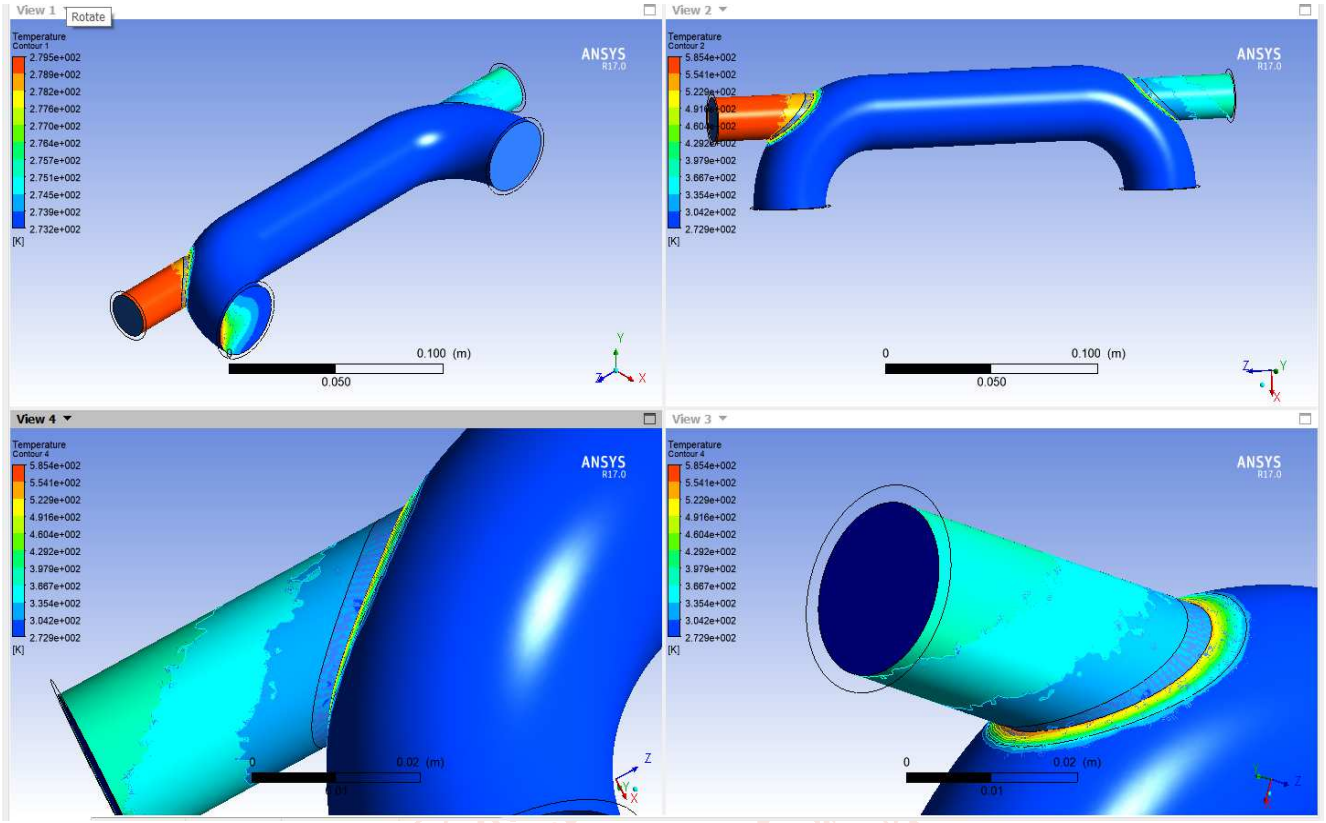

Figure 10 Temperature contour at Re = 25000 for heat exchanger using KNO_3–Ca $(NO3)_2$ + TiO2 molten salt nanofluid in a circular tube

- **For Re = 35000**

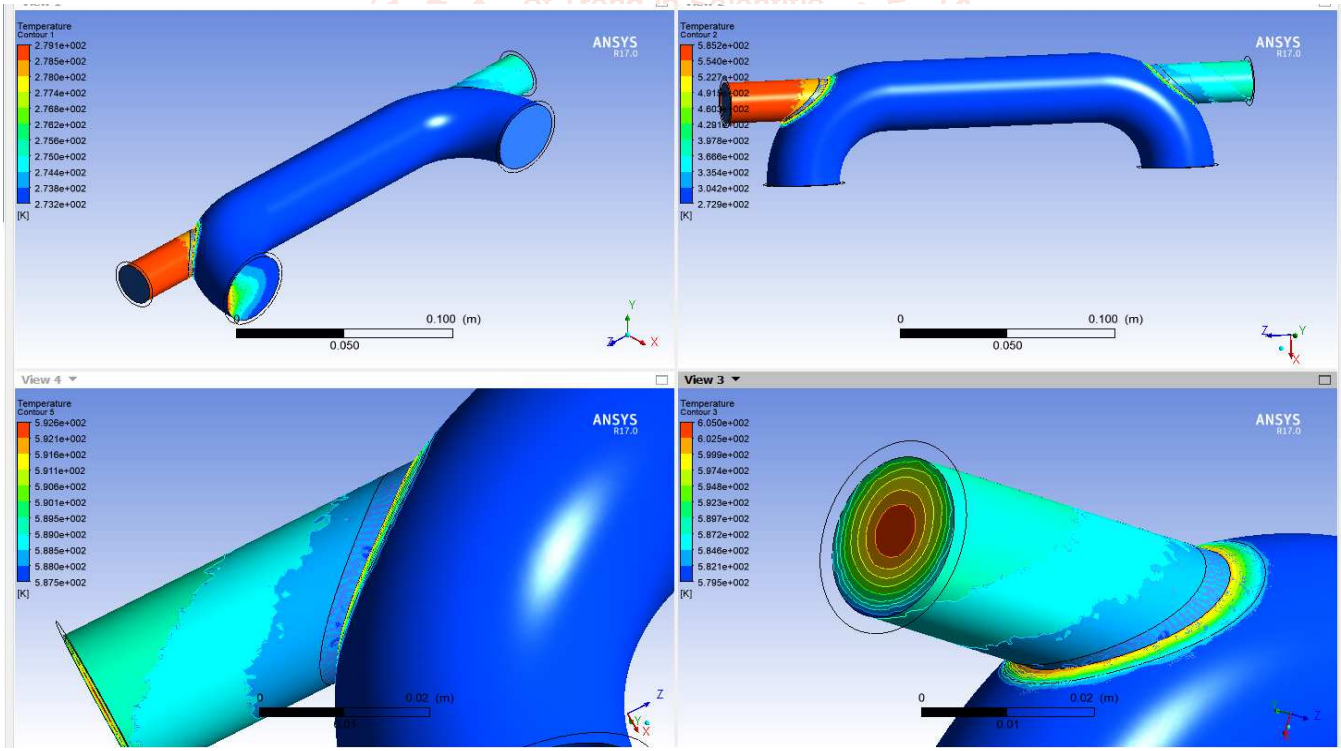

Figure 11. Temperature contour at Re = 35000 for heat exchanger using KNO_3–Ca $(NO3)_2$ + TiO2 molten salt nanofluid in a circular tube.

4.4. Comparison between Nanofluid fluid i.e. SiO2/Molten Salt and TiO2/Molten salt at different Reynold's number

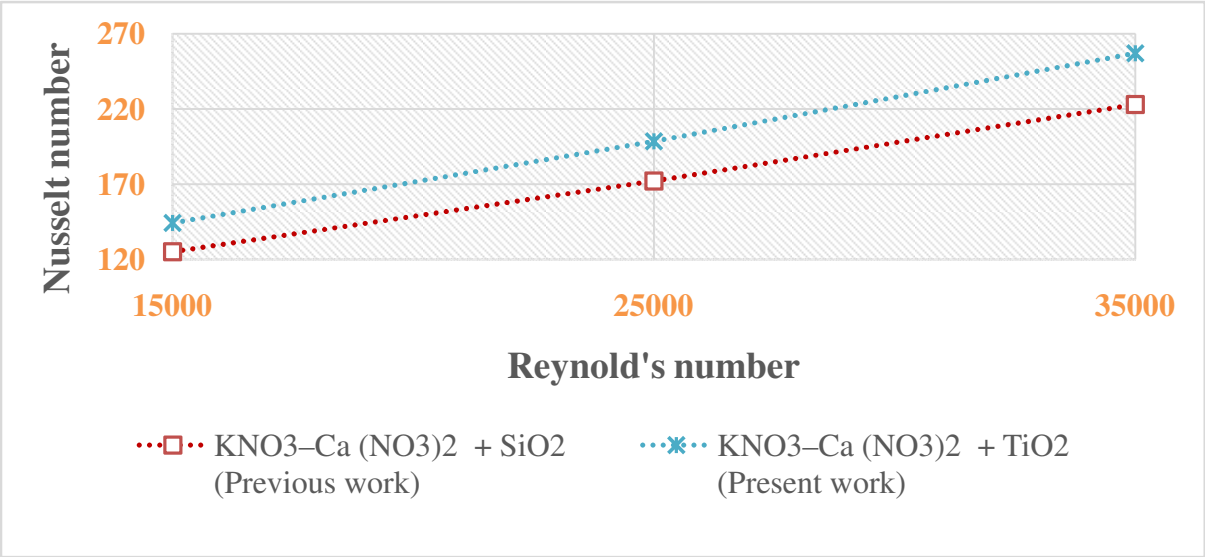

Figure 12 Nusselt number values comparison for Nanofluid fluid i.e. SiO_2/Molten Salt and TiO_2/Molten salt at different Reynold's number

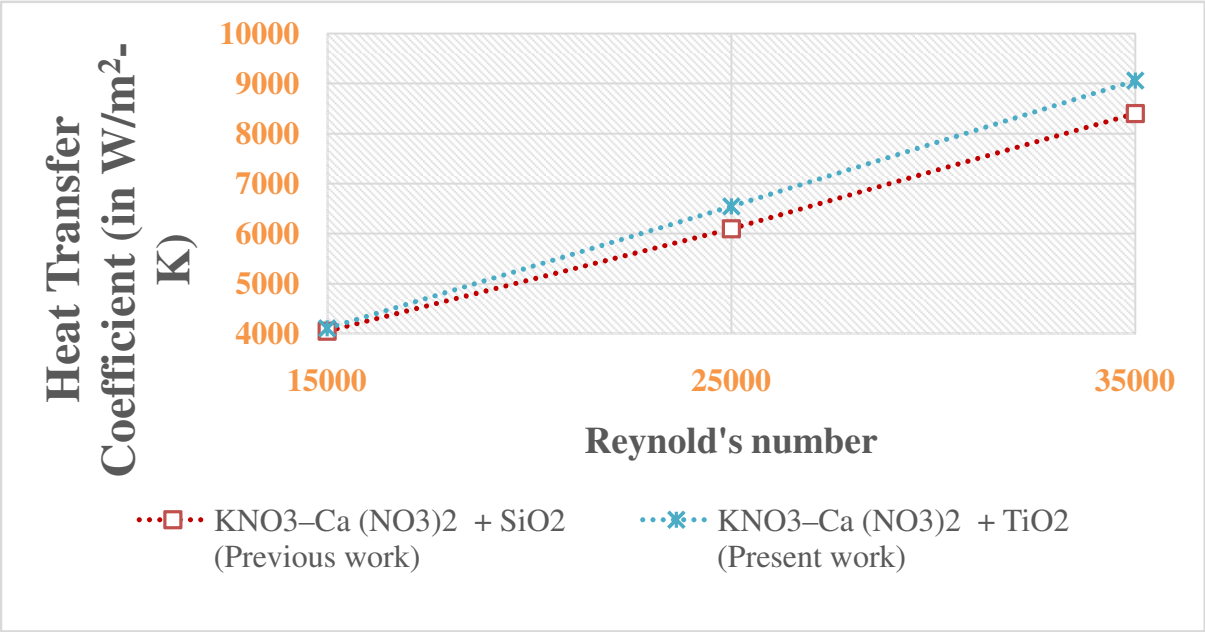

Figure 13 Heat transfer coefficient values comparison for Nanofluid fluid i.e. SiO_2/Molten Salt and TiO_2/Molten salt at different Reynold's number

V. CONCLUSIONS

This CFD research explores the thermal characteristics of KNO_3–Ca $(NO3)_2$+ TiO2 molten salt nanofluid in circular tube. A strong agreement has been seen in the comparison of the findings of this research with the existing experimental results of the literature. The effect of nanofluid were measured and observed to influence the heat transfer and flow of fluids in a heat exchanger. The following conclusions can be drawn based on the provided results:

- The KNO_3–Ca $(NO_3)_2$ + TiO_2 molten salt nanofluid performed slightly better in forced convection heat transfer than the KNO_3–Ca $(NO_3)_2$ + SiO_2 molten salt nanofluid under the same working conditions.
- KNO_3–Ca $(NO_3)_2$ + TiO_2 molten salt nanofluid had a 14.79 percent higher Nusselt number than KNO_3–Ca $(NO_3)_2$ + SiO_2 molten salt nanofluid.
- KNO_3–Ca $(NO_3)_2$ + TiO_2 molten salt nanofluid had a 7.880 percent higher heat transfer coefficient than KNO_3–Ca $(NO_3)_2$ + SiO_2 molten salt nanofluid.

REFERENCES

[1] Bin, L., Yu-Ting, W., Chong-fang, M., Meng, Y., Hang, G., 2009. Turbulent convective heat transfer with molten salt in a circular pipe. Int. Commun. Heat Mass Transf. 36, 912–916.

[2] Yang, M., Yang, X., Yang, X., Ding, J., 2010. Heat transfer enhancement and performance of the molten salt receiver of a solar power tower. Appl. Energy 87, 2808–2811.

[3] Lu, J., He, S., Ding, J., Yang, J., Liang, J., 2013. Convective heat transfer of high temperature molten salt in a vertical annular duct with cooled wall. Appl. Therm. Eng. 73, 1519–1524.

[4] Chen, Y. S., Wang, Y., Zhnag, J. H., Yuan, X. F., Tian, J., Tang, Z. F., Zhu, H. H., Fu, Y., Wang, N. X., 2016. Convective heat transfer characteristics in the turbulent region of molten salt in concentric tube. Appl. Therm. Eng. 98, 213–219.

[5] Du, B. -C., He, Y. -L., Wang, K., Zhu, H. -H., 2017. Convective heat transfer of molten salt in the shell-and-tube heat exchanger with segmental baffles. Int. J. Heat Mass Transf. 113, 456–465.

[6] Yanwei Hu, Yurong He, Zhenduo ZhangBaocheng Jiang, Yimin Huang., 2017. Natural convection heat transfer for eutectic binary nitrate salt based Al2O3 nanocomposites in solar power systems. Renewable Energy Volume 114, Part B, December 2017, Pages 686-696.

[7] Qian, J., Kong, Q. -L., Zhang, H. W., Zhu, Z. H., Huan, W. G., Li, W. H., 2017. Experimental study of shell-and-tube molten salt heat exchangers. Appl. Therm. Eng. 616–623.

[8] Chen, Y. S., Tian, J., Tang, Z. F., Zhu, H. H., Wang, N. X., 2018. Experimental study of heat transfer enhancement for molten salt with transversely grooved tube heat exchanger in laminar-transition-turbulent regimes. Appl. Therm. Eng. 132, 95–101.

[9] He, S., Lu, J., Ding, J., Yu, T., Yuan, Y., 2014. Convective heat transfer of molten salt outise the tube bundle of heat exchanger. Exp. Therm Fluid Sci. 59, 9–14.

[10] Hu Chena, Xia Chen, Yu-ting Wu, Yuan-wei Lu, Xin Wang, Chong-fang Ma, 2020. Experimental study on forced convection heat transfer of KNO3–Ca (NO3)2 + SiO2 molten salt nanofluid in circular tube. Solar Energy 206 (2020) 900–906.

[11] B. C. Pak, Y. L. Cho, Hydrodynamic and heat transfer study of Dispersed fluids with submicron metallic oxide particles, Exp. Heat Transf. 11 (1998) 151–170.

[12] H. E. Patel, K. B. Anoop, T. Sundararajan, Sarit K. Das, Model for thermal conductivity of CNT – nanofluids, Bull. Mater. Sci. 31 (3) (2008) 387–390.

[13] "Oak Ridge National Laboratory: Molten Salt Reactor," [Online]. Available: https://www.ornl.gov/msr.

[14] "Office of Energy Efficiency and Renewable Energy: Department of Energy," [Online]. Available: https://www.energy.gov/eere.

[15] Petukhov, B. S., 1970. Heat transfer and friction in turbulent pipe flow with variable physical properties. Adv. Heat Transf. 6, 503–564.

[16] Qian, J., Kong, Q. -L., Zhang, H. W., Zhu, Z. H., Huan, W. G., Li, W. H., 2017. Experimental study of shell-and-tube molten salt heat exchangers. Appl. Therm. Eng. 616–623.

[17] Qiu, Y., Li, M. -J., Wang, W. -Q., Du, B. -C., Wang, K., 2018. An experimental study on the heat transfer performance of a prototype molten-salt rod baffle heat exchanger for concentrated solar power. Energy 156, 63–72.

[18] Satoh, T., Yuki, K., Chiba, S. -Y., Hashizume, H., Sagara, A., 2017. Heat transfer performance for high prnadtl and high temperature molten slat flow in sphere-packed pipes. Fusion Sci. Technol. 52 (3), 618–624.

[19] Serrano-Lopez, R., Fradera, J., Cuesta-Lopez, S., 2013. Molten salts database for energy applications. Chem. Eng. Process. Process Intensif. 73, 87–102.

[20] Sieder, E. N., Tate, G. E., 1936. Heat transfer and pressure drop of liquids in tubes. Ind. Eng. Chem. 28, 1429–1435.

[21] Silverman, M. D., Huntley, W. R., Robertson, H. E., 1976. Heat transfer measurements in a forced convective loop with two molten flouride salts: LiF-BeF2-ThF2-UF4 and eutectic NaBF4-NaF. ORNL 5335.

[22] Smirnov, M., Khoklov, V. A., Filatov, E. S., 1987. Thermal Conductivity of Molten Alkali Halides and their mixtures. Electrochim. Acta 32 (7), 1019–1026.

[23] Sohal, m. S., Ebner, A. M., Sabharwall, P., Sharpe, P. "Engineering Database of Liquid salt Thermo physical and Thermo chemical Properties," Idaho National Laboratory, 2013.

[24] Wu, Y. -T., Chen, C., Liu, B., Ma, C. F., 2012. Investigation on forced convective heat transfer of molten salts in circular tubes. Int. Commun. Heat Mass Transf. 39, 1550–1555.

[25] Wu, Y. -T., Liu, S. -W., Xiong, Y. -X., Ma, C. -F., Ding, Y. -L., 2015. Experimental study on the heat transfer characteristics of a low melting point salt in a parabolic trough solar collector system. Appl. Therm. Eng. 89, 748–754.

[26] Xiao, P., Guo, L., Zhang, X., 2015. Investigations on heat transfer characteristic of molten salt flow in a helical annular duct. Appl. Therm. Eng. 88, 22–32.

[27] Yang, M., Yang, X., Yang, X., Ding, J., 2010. Heat transfer enhancement and performance of the molten salt receiver of a solar power tower. Appl. Energy 87, 2808–2811.

[28] Yu-Ting, W., Bin, L., Chong-Fang, M., Hang, G., 2009. Convective heat transfer in the laminar-turbulent transition region with molten salt in a circular tube. Exp. Therm Fluid Sci. 33, 1128–1132.